Cellulose (2018) 25:2143–2149
https://doi.org/10.1007/s10570-018-1730-6

COMMUNICATION

Isolation of oxidized nanocellulose from rice straw using the ammonium persulfate method

Ahmed A. Oun · Jong-Whan Rhim

Received: 19 August 2017 / Accepted: 27 February 2018 / Published online: 5 March 2018

Abstract Oxidized nanocellulose was isolated from rice straw using the ammonium persulfate method. The effect of cellulose isolation methods such as a multistep process, pretreatments using NaOH and H_2O_2 on the properties of the nanocellulose were studied. Oxidized cellulose nanofibrils showed long fibrils of the web-like structure with the diameter of 14 nm, while oxidized-cellulose nanocrystals displayed a needle shape with the length of 118–212 nm and the width of 12–19 nm depending on the isolation method of cellulose. Properties of the oxidized-nanocellulose such as shape, size, crystallinity, and thermal stability were influenced significantly by the cellulose isolation method.

Keywords Rice straw · Ammonium persulfate method · Oxidized nanocellulose

Introduction

Oxidized cellulose has been used in the biomedical and pharmaceutical applications due to their biodegradable, biocompatible, haemostatic, and antibacterial properties (Vendula and Miloslav 2013). Usually, an oxidized nanocellulose has been produced by using 2,2,6,6-tetramethylpiperidine-1-oxyl radical (TEMPO)-mediated oxidation method (Isogai et al. 2011), which can selectively oxidize primary hydroxyl groups of cellulose to carboxyl groups. Recently, ammonium persulfate (APS) method has been introduced as a one-step process for the production of oxidized-cellulose nanocrystals (CNC) (Cheng et al. 2014; Leung et al. 2011). The CNC produced by using the APS-oxidation method showed higher crystallinity, superior mechanical properties, and thermal stability compared with the cellulose nanofibrils (CNF) produced by the TEMPO-mediated oxidation method (Oun and Rhim 2017; Zhang et al. 2016).

Rice straw (RS) was used as a lignocellulosic resource due to its abundance, low cost, renewability, and reducing the agricultural waste (Harun and Geok 2016). For the isolation of nanocellulose from lignocellulosic sources, various chemical pretreatments are

Electronic supplementary material The online version of this article (https://doi.org/10.1007/s10570-018-1730-6) contains supplementary material, which is available to authorized users.

A. A. Oun
Food Engineering and Packaging Department, Food Technology Research Institute, Agricultural Research Center, Giza, Egypt

J.-W. Rhim (✉)
Center for Humanities, and Sciences and Department of Food and Nutrition, Kyung Hee University, 26 Kyungheedae-ro, Dongdaemun-gu, Seoul 02447, Republic of Korea
e-mail: jwrhim@khu.ac.kr

usually used to remove non-cellulosic materials such as lignin, hemicellulose, and extractives. Alkali treatment and bleaching using hydrogen peroxide (H_2O_2) were found to be an efficient pretreatment method with a relatively mild condition for the isolation of cellulose fiber by removing the hemicellulose and lignin from grain straws such as rice straw and barley straw (Harun and Geok 2016; Sun et al. 2002). Different isolation methods such as acid hydrolysis, mechanical, and TEMPO-oxidation methods with pre- or post-treatments have been used for the preparation of nanocellulose with various properties related to dimensions, morphology, thermal stability, crystallinity, and mechanical properties (Trache et al. 2017).

The main objective of the present study was to test the effect of cellulose isolation methods on the properties of rice straw nanocellulose prepared by the ammonium persulfate method.

Experimental method

Materials

Rice straw (RS) was collected from a local farm. Ammonium persulfate (APS $\geq$ 98%) was obtained from Sigma-Aldrich (St. Louis, MO, USA).

Extraction of cellulose

RS was cut into small pieces and washed with water and dried at 80 °C for 48 h, then ground to powders. Cellulose was extracted from the RS powder using three different methods. First, a conventional multistep purification method was used via removal of extractives, lignin, and hemicellulose according to the method of Lu and Hsieh (2012), which was designated as the multistep method. Second, the RS was pretreated with 6% NaOH at 60 °C for 2 h in the ratio of the RS to NaOH solution of 1:20 (w/v) (Harun and Geok 2016), which was designated as the NaOH method. Third, the RS was pretreated with 30% of H_2O_2 at 90 °C for 5 h in the ratio of the RS to H_2O_2 of 1:20 (w/v), which was designated as the H_2O_2 method (Chen et al. 2017). The procedure for the preparation of nanocellulose was schematically presented in Fig. 1. All of the resulting RS suspensions were washed with distilled water until the pH reached to 4–5, then dried in the oven at 60 °C overnight to get RS cellulose. The chemical composition of rice straw (α-cellulose, hemicelluloses, lignin, and extractives) was determined according to the quantitative analysis method (Oun and Rhim 2016).

Isolation of oxidized nanocellulose

Oxidized-CNF was isolated directly from the RS fiber (without any pre-treatment) using the method of Leung et al. (2011). Five grams of RS fiber was added to 500 mL of 1 M APS and stirred vigorously at 75 °C for 16 h. The reaction was stopped by washing the suspension with a distilled water until the pH reached around 4, then dispersed in 200 mL distilled water using an ultrasonic processor (Model VCX 750, Sonics & Materials Inc., New Town, CT, USA). Also, oxidized-CNC was isolated from the RS celluloses using the APS method as described above for the preparation of CNF (Fig. 1). The yield of CNF and CNC was determined by drying 50 mL of sample suspension at 60 °C and calculated based on the initial weight of the sample.

Characterization of morphology of nanocellulose

The morphology of the RS samples was observed using a field-emission scanning electron microscope (FE-SEM, S-4800, Hitachi Co., Ltd., Japan). The microstructure and dimension of nanocellulose were determined using a scanning transmission electron microscopy (STEM) using the FE-SEM with transmission mode. The length and diameter of samples were determined using the internal scale of the scanning transmission electron microscope (STEM), and the average values of 100 measurements in different points were presented.

Evaluation of chemical structure

FTIR spectra of fiber samples were obtained using an attenuated total reflectance-Fourier transform infrared (ATR-FTIR) spectrophotometer (TENSOR 37 Spectrophotometer, Billerica, MA, USA). Dried samples were ground and pelletized using KBr (1:100 w/w), and their spectra were recorded at 4000–400 cm^{-1}.

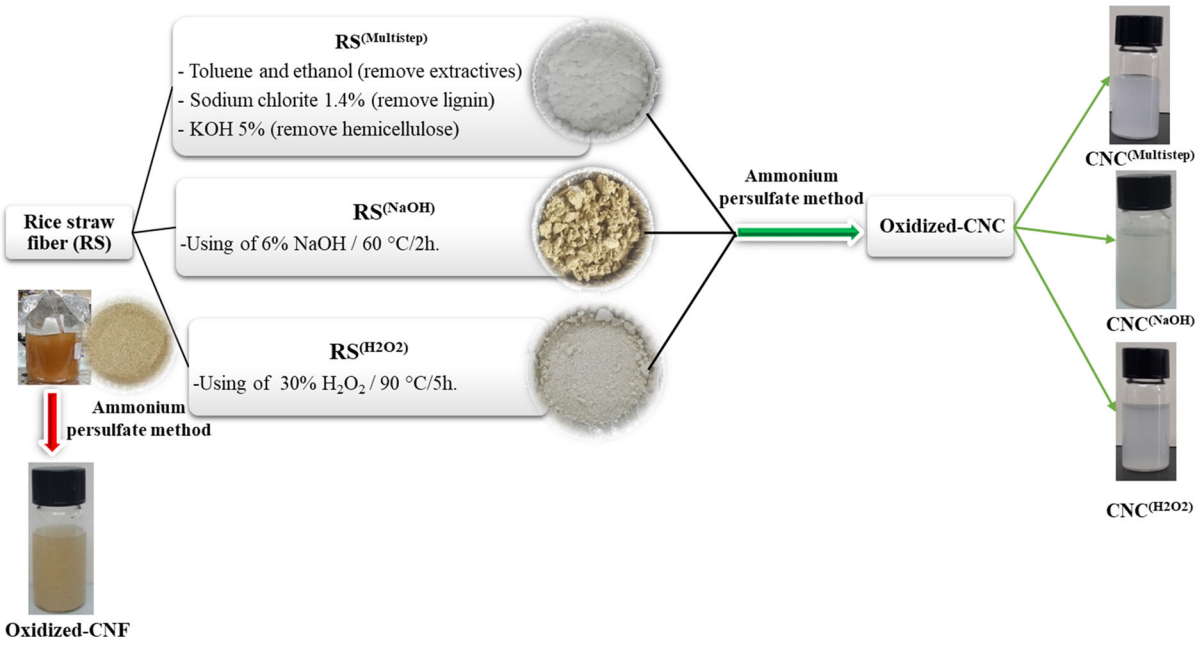

Fig. 1 Procedures for the isolation of oxidized-nanocellulose

Crystallinity properties

X-ray diffraction (XRD) patterns of samples were analyzed using an XRD diffractometer (PANalytical Xpert pro MRD diffractometer, Amsterdam, Netherlands), which operated at 40 kV and 30 mA, with a Cu Kα radiation at a wavelength of 1.54056 Å. The crystallinity index (CI) of samples was calculated using the following equation (Park et al. 2010):

$$\mathrm{CI} = \frac{\mathrm{I}_{200} - \mathrm{I}_{am}}{\mathrm{I}_{200}} \times 100 \quad (1)$$

where I_{200} and I_{am} represent the maximum peak intensity at around $2\theta = 21.7°$ and the minimum intensity between the planes (200) and (110), respectively.

Thermal stability of the samples was evaluated using a thermogravimetric analyzer (Hi-Res TGA 2950, TA Instrument, New Castle, DE, USA). About 10 mg of the samples were heated from 30 to 600 °C under a nitrogen flow of 50 cm^3/min at a heating rate of 10 °C/min.

Results and discussion

Morphology of nanocellulose

The RS was composed of 36.5 ± 2.1% α-cellulose, 38.0 ± 1.6% hemicellulose, 22.0 ± 2.7% lignin, and 3.5 ± 1.9% extractives, which were consistent with previously reported results (Oun and Rhim 2016). Apparently, the ground fiber of the RS was yellowish-brown (Fig. 2). After APS treatment, the RS suspension turned into light-yellow, which was probably due to the partial removal of lignin via the free radicals ($SO_4^{\cdot-}$), hydrogen peroxide (H_2O_2), and HSO_4^- produced during the APS treatment (Leung et al. 2011). However, the RS cellulose prepared by the multistep method was white, which was due to the removal of extractives, lignin, and hemicellulose. The RS cellulose obtained by the pretreatment with NaOH showed yellowish time, which might be due to the insufficient removal of hemicellulose and lignin (Sun et al. 2000). The RS cellulose obtained by the pretreatment with H_2O_2 was more white, which was probably due to the oxidative degradation of phenolic compounds or lignin by the H_2O_2 (Sun et al. 2000, 2002). On the other hand, all the CNC isolated from the RS cellulose showed white suspensions after the APS oxidation.

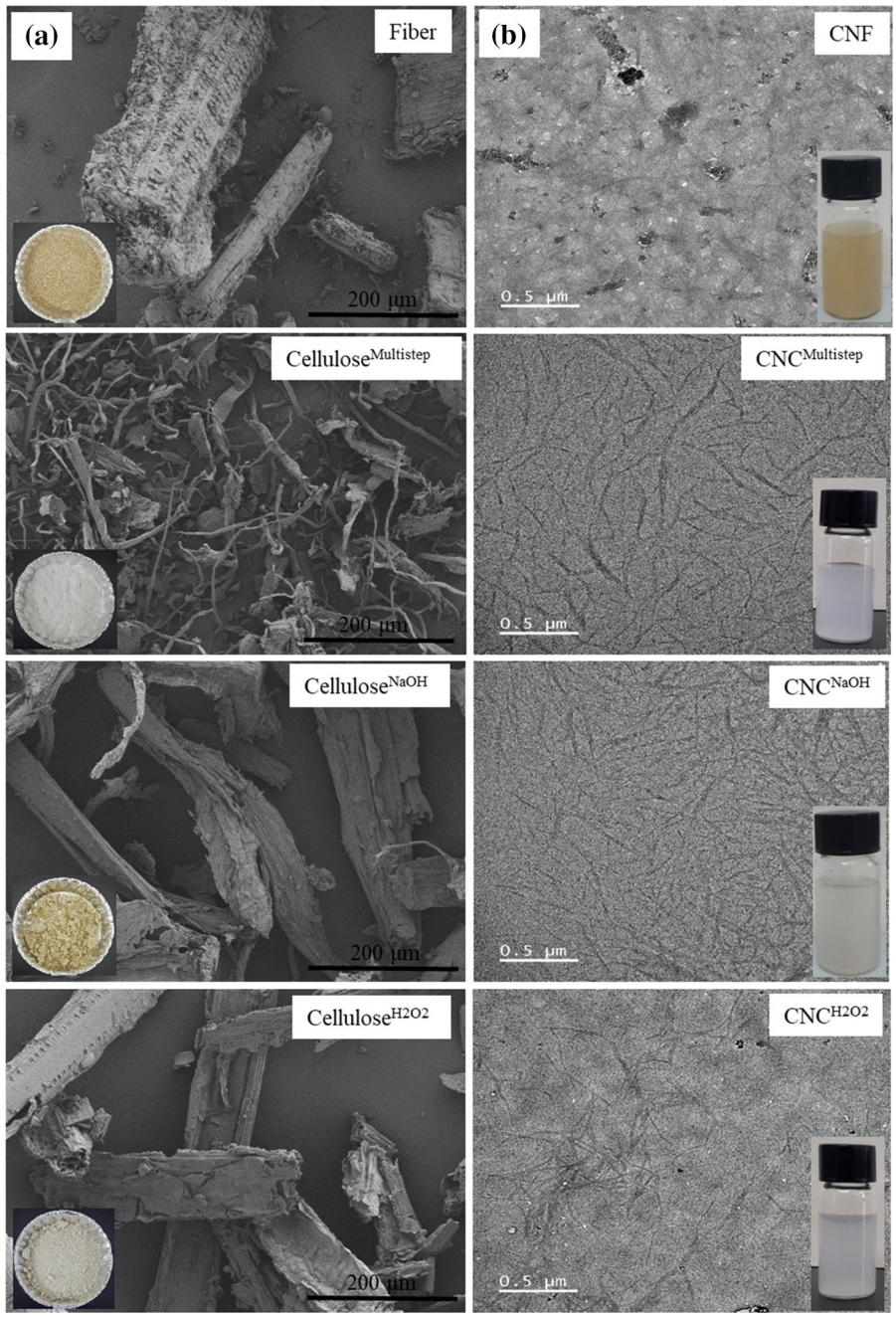

Fig. 2 **a** SEM images of RS fiber and cellulose **b** TEM images of nanocellulose

The particle size of the RS fibers was 459 ± 180 µm in length (L) and 85 ± 62 µm in width (W) (Fig. 2a). After the multistep extraction, pretreatments with NaOH and H_2O_2, the size decreased to (L = 184 ± 89 µm and W = 15 ± 6.5 µm) (L = 302 ± 73 µm and W = 68 ± 29 µm), and (L = 428 ± 145 µm and W = 72 ± 16 µm), respectively. The cellulose prepared by the multistep process was the smallest, presumably due to the removal of most of the extractives, hemicellulose, and lignin.

The CNF obtained by the APS method was composed of long fibrils of the web-like structure with a diameter of 14 ± 7.0 nm. However, the CNC isolated by the multistep method and pretreatments with NaOH and H_2O_2 formed a needle shape with the length of 118 ± 52, 137 ± 64, and 212 ± 80 nm, and the diameter of 19 ± 5, 12 ± 5, and 16 ± 8 nm, respectively. Particles size distribution histograms and STEM images of CNF and CNC determined as shown in the supporting information (S1, S2). The decreased size of the CNC was attributed to the removal of not only amorphous regions but also lignin and hemicellulose by the APS treatment (Leung et al. 2011). Elazzouzi-Hafraoui et al. (2008) reported that the length and width of CNC were affected by the isolation methods of CNC as well as the source of cellulose. Also, a pulp pretreated with drying at 110 °C produced shorter CNC compared with those without drying pre-treatment (Kontturi and Vuorinen 2009). The average yield of CNF, $CNC^{Multistep}$, CNC^{NaOH}, and CNC^{H2O2} samples was 25.6 ± 2.1, 34 ± 1.8, 27.5 ± 1.5, and 28 ± 1.1%, respectively. CNF showed the lowest yield, which may be due to partial removal of the hemicellulose and lignin by the APS method (Leung et al. 2011). Compared to CNF, the yield of CNCs increased due to the removal most of the hemicellulose, lignin, and extractive by the multistep purification and pretreatment with NaOH or H_2O_2 (Harun and Geok 2016). Jiang and Hsieh (2013) reported that the yields of nanocellulose materials isolated from rice straw cellulose by the mechanical, the TEMPO-oxidation, and the sulfuric acid hydrolysis were 12, 19.7, and 16.9%, respectively. Whereas the yields of nanocellulose materials were significantly affected by isolation methods and isolation conditions such as reaction time and temperature.

The FTIR spectra of the RS fiber, cellulose, CNF, and CNC are shown in Fig. 3a. RS fibers showed peaks at 3343 cm^{-1} (O–H stretching vibrations), 2919 cm^{-1} (C–H), 1728 cm^{-1} (C=O) of xylan component in hemicellulose, 1516 cm^{-1} (aromatic ring vibrations) of lignin, 1421 and 898 cm^{-1} of cellulose, and 785 cm^{-1} of silica (Lu and Hsieh 2012). After the multistep treatment, the peaks of hemicellulose, lignin, and silica disappeared (Oun and Rhim 2016). The shift of peak at 1640 cm^{-1}, (O–H vibration) to 1618 cm^{-1} was probably due to the introduction of carboxylic groups into C6 hydroxyl group of cellulose after H_2O_2 pretreatment (Chen et al. 2017). While the RS cellulose obtained by NaOH pretreatment showed only a small peak of lignin without peaks of hemicellulose and silica.

After the APS treatment, all the nanocellulose showed a peak at 1728 cm^{-1} due to the introduction of a carboxyl group (Cheng et al. 2014). Peaks of hemicellulose and lignin in the cellulose obtained by the pretreatments with NaOH and H_2O_2 were disappeared after the APS process (Leung et al. 2011).

XRD analysis

XRD diffraction patterns of the RS fiber, cellulose, CNF, and CNC are shown in Fig. 3b. The intensity of XRD peaks of the RS fiber at around 2θ = 15.8° (110) and 2θ = 22.3° (200) increased after chemical treatment, which indicated the increase in the crystallinity due to the removal of non-cellulosic materials and amorphous regions by the APS treatment (Leung et al. 2011; Oun and Rhim 2016). The CI of RS cellulose calculated using Eq. (1) increased from 39.5% to 54.2, 50.6, and 47.4% after the multistep extraction and pretreatments with NaOH and H_2O_2, respectively. The CI of CNF was 41.3% and those of CNC were 49.3, 58.4, and 30.1% for the CNC isolated by the multistep extraction and the pretreatments with NaOH and H_2O_2, respectively. The CI of the CNC produced by the NaOH treatment was higher than that produced by the H_2O_2 treatment, which was presumably due to the formation of more carboxyl groups in the latter.

Thermal stability analysis

The TGA thermograms of the RS fiber and cellulose showed two main steps of weight loss (Fig. 4a). The first change was observed at 60–120 °C with a weight loss of 1–3.2%, which was due to the evaporation of water (Oun and Rhim 2016). The main weight loss was observed at 200–400 °C, which was due to the thermal degradation of cellulosic and non-cellulosic materials (Jiang and Hsieh 2013). The RS cellulose obtained by the multistep process showed the highest onset decomposition temperature (T_{onset}; 265 °C). The T_{onset} of RS $cellulose^{NaOH}$ (242 °C) was higher than that of the RS fiber (230 °C), which was probably due to the partial removal of hemicellulose and lignin. The T_{onset} of the RS $cellulose^{H2O2}$ was the lowest (212 °C), which was due to the introduction of carboxyl groups.

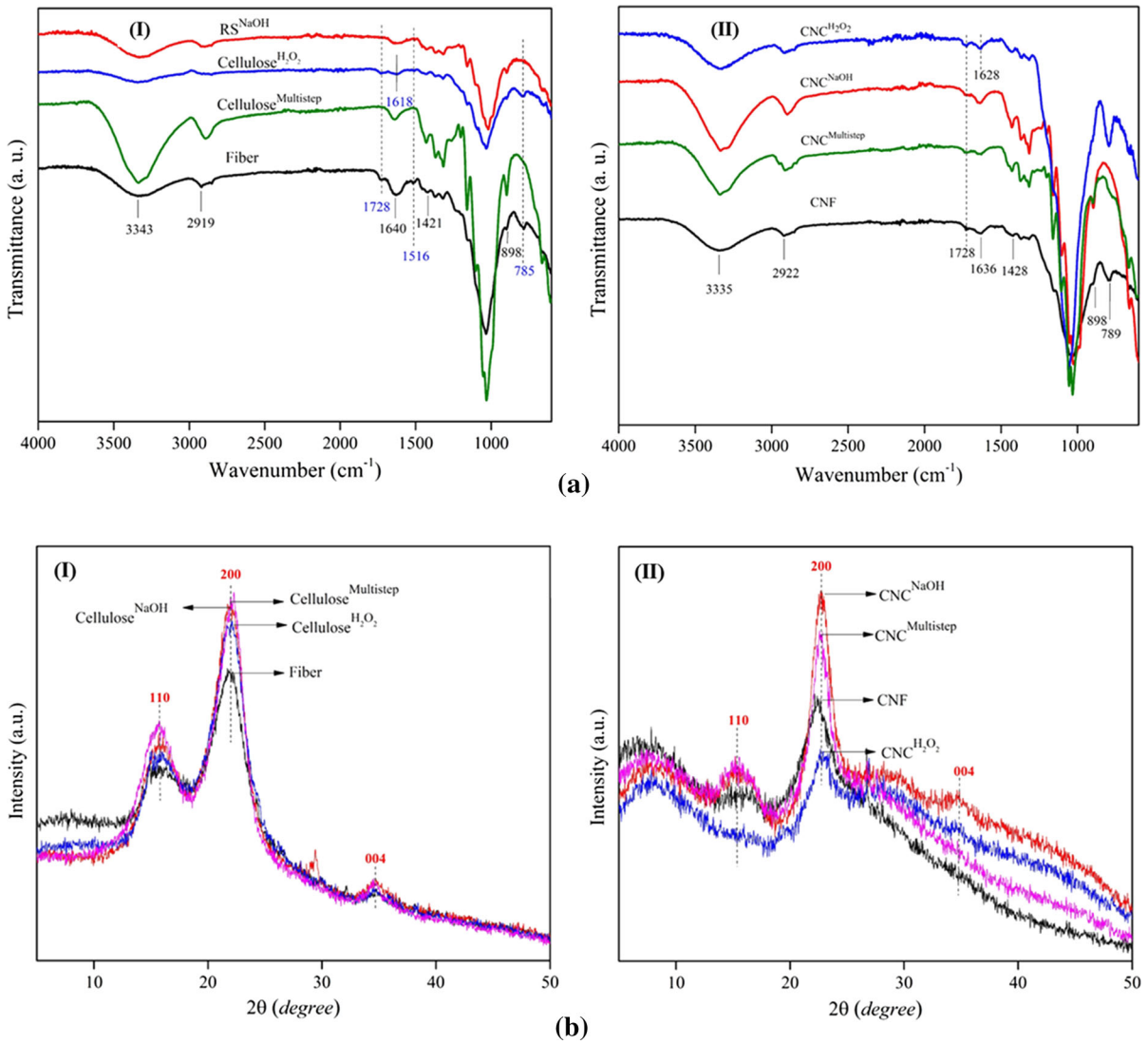

Fig. 3 **a** FTIR spectra of (I) fiber and cellulose (II) nanocellulose, **b** XRD spectra of (I) fiber and cellulose (II) nanocellulose

Figure 4b shows the effect of APS treatment on the properties of isolated cellulose. The T_{onset} of all the nanocellulose decreased significantly, which was probably due to the increased heat transfer rate as a result of the increased surface area with smaller particle sizes of the nanocellulose and introduction of carboxyl groups (Jiang and Hsieh 2013; Zhang et al. 2016). However, the thermal stability of the nanocellulose might be higher than the CNC prepared using the commonly used sulfuric acid hydrolysis method due to the introduction of sulfate ester groups (Roman and Winter 2004).

Conclusion

Cellulose was extracted from rice straw using a multistep extraction and pretreatments with alkali and hydrogen peroxide. Oxidized nanocellulose were isolated from the cellulose using an ammonium persulfate method. The nanocellulose obtained from the cellulose pretreated with NaOH showed the highest crystallinity. Properties of the oxidized nanocellulose can be tuned by using different cellulose extraction methods for the food packaging and biomedical applications.

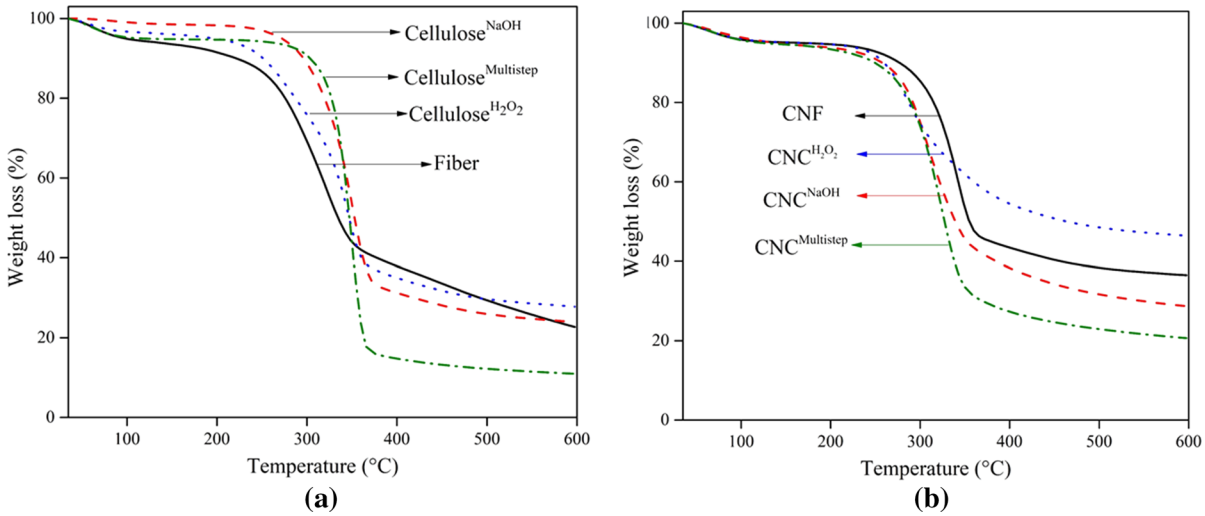

Fig. 4 TGA thermograms of **a** fiber and cellulose **b** nanocellulose

Acknowledgments This research was supported by the Agriculture Research Center (ARC 710003) program of the Ministry of Agriculture, Food and Rural Affairs, Korea.

References

Chen YW, Lee HV, Hamid SBA (2017) Facile production of nanostructured cellulose from Elaeis guineensis empty fruit bunch via one pot oxidative-hydrolysis isolation approach. Carbohyd Polym 157:1511–1524

Cheng M, Qin Z, Liu Y, Qin Y, Li T, Chen L, Zhu M (2014) Efficient extraction of carboxylated spherical cellulose nanocrystals with narrow distribution through hydrolysis of lyocell fibers by using ammonium persulfate as an oxidant. J Mater Chem A 2:251–258

Elazzouzi-Hafraoui S, Nishiyama Y, Putaux J-L, Heux L, Dubreuil F, Rochas C (2008) The shape and size distribution of crystalline nanoparticles prepared by acid hydrolysis of native cellulose. Biomacromol 9:57–65

Harun S, Geok SK (2016) Effect of sodium hydroxide pretreatment on rice straw composition. Indian J Sci Technol 9:1–21

Isogai A, Saito S, Fukuzumi H (2011) TEMPO-oxidized cellulose nanofibers. Nanoscale 3:71–85

Jiang F, Hsieh YL (2013) Chemically and mechanically isolated nanocellulose and their self-assembled structures. Carbohyd Polym 95:32–40

Kontturi E, Vuorinen T (2009) Indirect evidence of supramolecular changes within cellulose microfibrils of chemical pulp fibers upon drying. Cellulose 16:65–74

Leung ACW, Hrapovic S, Lam E, Liu Y, Male KB, Mahmoud KA, Luong JHT (2011) Characteristics and properties of carboxylated cellulose nanocrystals prepared from a novel one-step procedure. Small 7:302–305

Lu P, Hsieh Y-L (2012) Preparation and characterization of cellulose nanocrystals from rice straw. Carbohyd Polym 87:564–573

Oun AA, Rhim JW (2016) Isolation of cellulose nanocrystals from grain straws and their use for the preparation of carboxymethyl cellulose-based nanocomposite films. Carbohyd Polym 150:187–200

Oun AA, Rhim J-W (2017) Characterization of carboxymethyl cellulose-based nanocomposite films reinforced with oxidized nanocellulose isolated using ammonium persulfate method. Carbohyd Polym 174:484–492

Park S, Baker JO, Himmel ME, Parilla P, Johnson DK (2010) Cellulose crystallinity index: measurement techniques and their impact on interpreting cellulase performance. Biotechnol Biofuels 3(1):10–20

Roman M, Winter WT (2004) Effect of sulfate groups from sulfuric acid hydrolysis on the thermal degradation behavior of bacterial cellulose. Biomacromolecules 5:1671–1677

Sun RC, Tomkinson J, Ma PL, Liang SF (2000) Comparative study of hemicelluloses from rice straw by alkali and hydrogen peroxide treatments. Carbohyd Polym 42:111–122

Sun RC, Sun XF, Fowler P, Tomkinson J (2002) Structural and physico-chemical characterization of lignins solubilized during alkaline peroxide treatment of barley straw. Eur Polymer J 38:1399–1407

Trache D, Hussin MH, Haafiz MKM, Thakur VK (2017) Recent progress in cellulose nanocrystals: sources and production. Nanoscale 24:17–25

Vendula H, Miloslav M (2013) Oxidized cellulose with different carboxyl content: structure and properties before and after beating. Phys Procedia 44:256–261

Zhang K, Sun P, Liu H, Shang S, Song J, Wang D (2016) Extraction and comparison of carboxylated cellulose nanocrystals from bleached sugarcane bagasse pulp using two different oxidation methods. Carbohyd Polym 138:237–243